CHEMMEDCHEM

CHEMISTRY ENABLING DRUG DISCOVERY

Accepted Article

Title: Investigating structural requirements for the antiproliferative activity of biphenyl nicotinamides

Authors: Cosimo Damiano Altomare, Maria Majellaro, Angela Stefanachi, Piero Tardia, Chiara Vicenti, Angelina Boccarelli, Alessandra Pannunzio, Federica Campanella, Mauro Coluccia, Nunzio Denora, Francesco Leonetti, Modesto de Candia, and Saverio Cellamare

To be cited as: *ChemMedChem* 10.1002/cmdc.201700365

Link to VoR: http://dx.doi.org/10.1002/cmdc.201700365

A Journal of

ChemPubSoc Europe

WILEY-VCH

www.chemmedchem.org

FULL PAPER WILEY-VCH

Investigating structural requirements for the antiproliferative activity of biphenyl nicotinamides

Maria Majellaro,[a]§ Angela Stefanachi,[a]§ Piero Tardia,[b] Chiara Vicenti,[c] Angelina Boccarelli,[d] Alessandra Pannunzio,[a] Federica Campanella,[a] Mauro Coluccia,[a] Nunzio Denora,[a] Francesco Leonetti,[a] Modesto de Candia,[a] Cosimo Damiano Altomare,*[a] and Saverio Cellamare[a]

[a] M. Majellaro, Dr. A.Stefanachi, Dr. A. Pannunzio, F. Campanella, Prof. M. Coluccia, Prof. N. De Nora, Dr. M.de Candia, Prof. S. Cellamare, Prof. C. D. Altomare.
Department of Pharmacy-Drug Sciences, University of Bari, Via Orabona 4, 70125, Bari, Italy.
E-mail: cosimodamiano.altomare@uniba.it
[b] Dr. P. Tardia.
D3-Drug Discovery and Development Department, Istituto Italiano di Tecnologia, Via Morego 30, 16163 Genova, Italy
[c] Dr. C. Vicenti.
Department of Emergency and Organ Transplantation, Section of Pathological Anatomy, University of Bari, Piazza Giulio Cesare 11, Bari, Italy. 70124.
[d] Dr. A. Boccarelli.
Department of Biomedical Sciences and Human Oncology, University of Bari, Piazza Giulio Cesare 11, Bari, Italy. 70124.
[§] These authors equally contributed to the work.

Abstract: A number of trimethoxybenzoic acid anilides, previously studied as P-gp (permeability glycoprotein) modulators, were screened with the aim of identifying new anticancer agents. One of these compounds, which showed antiproliferative activity against resistant MCF-7 cell line, was selected as the hit structure. The replacement of the trimethoxybenzoyl moiety with the nicotinoyl one, for overcoming solubility issues, led to synthesize a new series of *N*-biphenyl nicotinoyl anilides, among which a nitro derivative (**3**) displayed antiproliferative activity against MCF7 and MDA-MB231 cells in the nanomolar range. Searching for a bioisoster of the NO_2 group led to a nitrile analogue (**36**) showing a strong increase in activity against MCF-7 and MDA-MB231 cells. Compound **36** induced on MCF7 cells a dose-dependent accumulation of G2- and M-phase cell populations and a decrease of S-phase cells. Compared to vinblastine, a well known potent antimitotic agent, compound **36** induced also a G1 arrest at low doses (20-40 nM), but did not inhibit *in vitro* tubulin polymerization.

Introduction

The discovery of novel small molecule modulating processes critically involved in the growth and survival of human tumors, is one of the major challenges in oncological drug discovery research.[1] Many organizations, both private and public, have heavily invested in HTS (high throughput screening) campaigns of libraries of thousands-to-millions compounds.[2]

Some years ago, our research group started a medium-screening program of in-house focused chemical libraries aimed at identifying new molecules with antiproliferative activity, first evaluating a set of newly synthesized P-gp (permeability glycoprotein) modulators.[3,4] Multidrug resistance (MDR), which is among the main causes of chemotherapy failure, is unrelated to the pharmacological activity of drugs and could be triggered by diverse mechanisms, including drug metabolism acceleration, apoptotic pathway modulation, cellular damage repair and drug efflux pump (e.g., P-gp) overexpression.[5]

Most of the investigated substances were biphenyl anilides of trimethoxy benzoic acids, whose ability to modulate P-gp was found to correlate with lipophilicity.[4] The most lipophilic compounds, especially those able to form an intramolecular hydrogen bond (IMHB), such as compound **1** (Figure 1), showed submicromolar IC_{50} values against P-gp, but their poor aqueous solubility hampered a hit-to-lead development.[4] Interestingly, compound **1**, which displayed a nanomolar affinity to P-gp, also showed intrinsic cytotoxicity towards MCF7-adr cell line resistant to doxorubicin.[4]

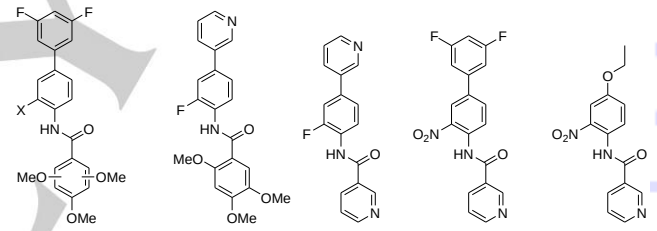

Figure 1. Structural modifications leading to hit identification.

This evidence prompted us to screen the antiproliferative activity of a series of trimethoxy and non-trimethoxy anilides (Table 1). Due to their poor aqueous solubility, these compounds were tested at a maximum concentration of 2.5 μM, but none of them showed effects against MCF7 and MDA-MB-231 cell lines. To improve the solubility, the nicotinamide derivative **2** (Figure 1) was synthesized as a strict analog of **1**, but despite its higher solubility it showed decreased P-gp affinity and loss of antiproliferative effects.[4]

The nicotinamide moiety can be considered a privileged scaffold, because of diverse biological activities shown by the large amount of bioactive substances incorporating this fragment. Representative examples of bioactive nicotinoyl derivatives are shown in Figure 2, which includes the *N*-phenyl nicotinoyl derivative **16** as human sirtuin-2-selective inhibitor,[7] **17** as sodium channel blocker,[8] **18** as soluble epoxide hydrolase inhibitor,[9] **19** as HDAC1/HDAC2 inhibitor,[10] **20** as anti-leishmanial agent,[11] and **21** as aquaporin 4 inhibitor.[12] The *N*-biphenyl-4-ylnicotinamide analog of **21**, which may be considered as a template of the compounds investigated herein, proved to be active against a panel of bioassays, such as HIV-1

RNase H inhibition, MKP-3, HePTP, Hsp70, ER stress-induced cell death and VHR1 *in vitro* high throughput screening.[13]

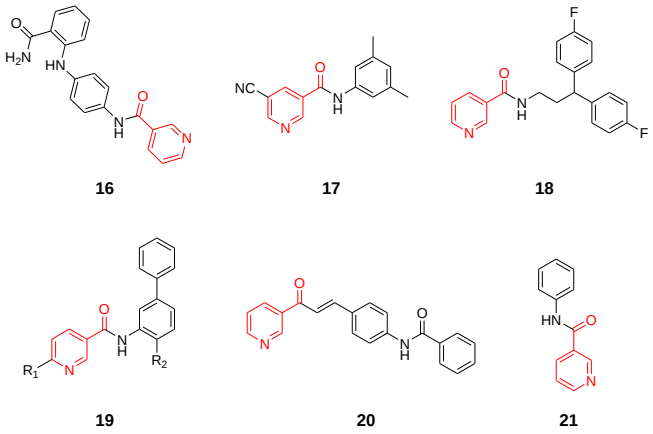

Figure 2. Representative bioactive compounds bearing *N*-phenyl nicotinoyl moiety.

Herein we report the synthesis of a new series of *N*-biphenyl nicotinoyl anilides and evaluation of their antiproliferative activity against MCF7 and MDA-MB231 cell lines. A starting point of this study was that the *ortho*-nitro biphenyl derivative **3** showed antiproliferative activity against MCF7 and MDA-MB231 cell lines in the nanomolar range of concentrations. This result was somehow supported by the activity reported by others for the *ortho*-nitrophenyl analog **4** (Figure 1), which acts as an apoptosis inducer identified by caspase-based HTS assay.[6]

The search of the structural requirements for maintaining (or increasing) the antiproliferative activity of the biphenyl nicotinamide derivative **3** was carried out by synthesizing and testing (i) the positional isomers (isonicotinamide and picolinamide) and a few different congeners (substituents on the distal phenyl of the biphenyl moiety), and (ii) the bioisosteric replacement of the *ortho*-NO_2 group.

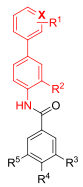

Cpd[a]	X	R^1	R^2	R^3	R^4	R^5
5	C	3,5-diF	NO_2	OCH_3	OCH_3	H
6	C	3,5-diF	NO_2	OCH_3	H	OCH_3
7	C	3,5-diF	NO_2	H	H	H
8	C	3,5-diF	NO_2	F	F	F
9	C	3,5-diF	NO_2	OCH_2O		H
10[4]	N	-	F	H	H	H
11	C	3-F	NO_2	OCH_3	OCH_3	OCH_3
12[4]	C	3,5-diF	NH_2	OCH_3	OCH_3	OCH_3
13	C	3,5-diF	NH_2	F	F	F
14[3]	C	3-$COCH_3$	NO_2	OCH_3	OCH_3	OCH_3
15[3]	N	-	NO_2	OCH_3	OCH_3	OCH_3

Table 1. Previously and newly synthesized biphenyl benzamide derivatives lacking antiproliferative activity against MCF7 and MDA-MB-231 cell lines at 2.5 μM concentration. [a] Synthesis details and analytical data in the references reported in squared brackets.

Results and Discussion

The newly investigated biphenyl nicotinamide derivatives were synthesized following the synthetic pathways shown in Schemes 1 and 2. Structural details along with the antiproliferative activities, expressed as IC_{50} values, are reported in Tables 2 and 3. A number of newly and previously synthesized derivatives showing no activity at 2.5 μM (solubility limit in the assay conditions for most of them) are shown in Table 1.

The first step of the synthesis consisted in a Suzuki reaction between the suitable aniline and the aryl boronic acid to obtain the biphenyl aniline derivatives **1A**-**11A** (Scheme 1). Then, a condensation between the biphenyl aniline and nicotinoyl chloride or trimethoxybenzoylchloride, in dry dioxane in the presence of DMAP and TEA, yielded compounds **24**-**27**, **29**-**31**, **33**-**34**, **36** and **37**. Compounds **3**, **22** and **23** were synthesized by reacting 3',5'-difluoro-3-nitro-[1,1'-biphenyl]-4-amine **1A** with nicotinoyl chloride, picolinoyl chloride and isonicotinoyl chloride, respectively. Compound **36** and **37** were prepared by condensation of 4-amino-4'-fluoro-[1,1'-biphenyl]-3-carbonitrile **11A** with nicotinoyl chloride (**36**) or 3,4,5-trimethoxybenzoyl chloride (**37**). Compound **32** was synthesized through hydrolysis of **31** (Scheme 1).

A Suzuki reaction between the commercially available 5-chloro-2-nitroaniline and 4-fluorobenzenboronic acid, carried out in the above conditions, led to **12A**, which yielded **28** after condensation with nicotinoyl chloride. To prepare compound **35**, the biphenylaniline **12A** first underwent acetylation of the NH_2 group (**13A**) and next a reduction to NH_2. The biphenyl aniline intermediate **14A** was reacted with nicotinoyl chloride to yield compound **35** (Scheme 2).

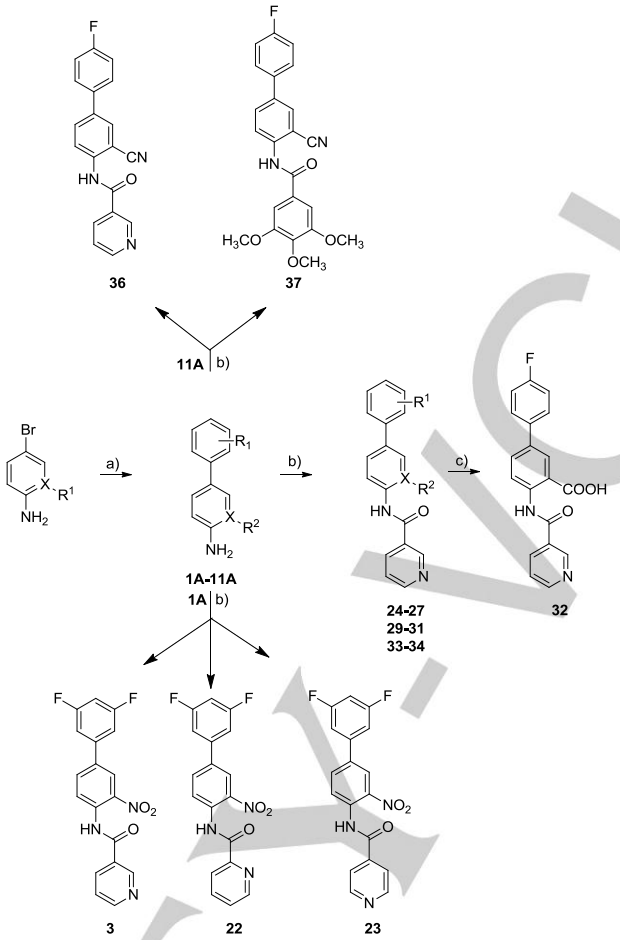

Scheme 1.

Reagents and conditions: a) aryl boronic acid, dioxane, 2M K_2CO_3, $Pd(PPh_3)_4$, reflux; b) aryloyl chloride, dry dioxane, DMAP, Et_3N, reflux c) LiOH, THF/H_2O r.t.

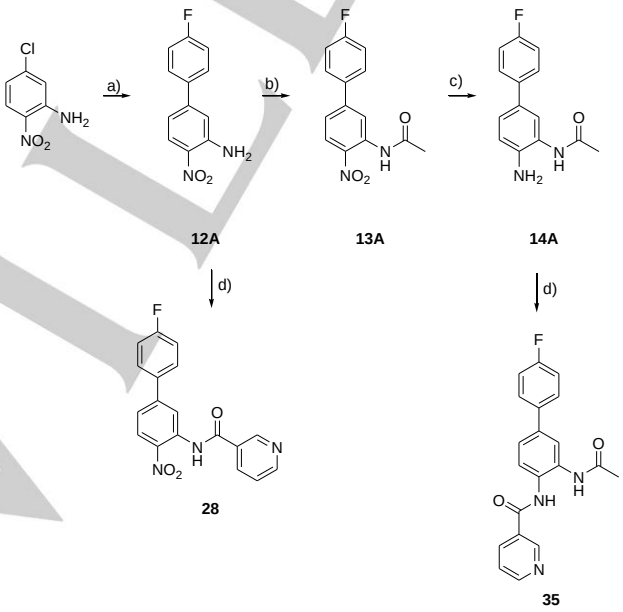

Scheme 2.

Reagents and conditions: a) aryl boronic acid, dioxane, $Pd(PPh_3)_4$, K_2CO_3 2M, reflux; b) CH_3COCl, THF, r.t.; c) $SnCl_2$ MeOH; d) nicotinoyl chloride, dioxane, DMAP, Et_3N, reflux.

General structure	cpd	X^2	X^3	X^4	R^1	R^2	R^3	R^4	MCF7 (IC_{50} nM)[a]	MDA-MB231 (IC_{50} nM)[a]	log k'[b]
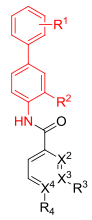	**3**	C	N	C	3',5'-diF	NO_2	-	H	250±70	229±95	0.89±0.01
	4[6]	C	N	C	[c]	NO_2	-	H	100±70	200±90	-
	22	N	C	C	3',5'-diF	NO_2	H	H	> 2500	> 2500	1.61±0.01
	23	C	C	N	3',5'-diF	NO_2	H	-	> 2500	> 2500	0.94±0.01
	24	C	N	C	4'-F	NO_2	-	H	58±10	32±3	0.78±0.01
	25	C	N	C	3'-F	NO_2	-	H	325±150	68±50	0.79±0.01
	26	C	N	C	4'-OCH_3	NO_2	-	H	1400±500	> 2500	0.76±0.01
	27	C	N	C	3'-OCH_3	NO_2	-	H	30±10	30±10	0.80±0.01
	28	C	N	C	[d]	NO_2	-	H	450±200	> 2500	0.80±0.01
CA4[e]		-	-	-	-	-	-	-	4.85±1.6	3.3±0.47	-
Cisplatin		-	-	-	-	-	-	-	2730±1500	1000±150	-

Table 2. Antiproliferative activity data (IC_{50}) against MCF7 and MDA-MB231 cell lines of R_1-substituted *ortho*-nitro-biphenyl nicotinamides and positional isomers. [a] IC_{50} values (nM) coming from the mean of at least three independent experiments ± SEM, sampled in triplicate. [b] Log of the capacity factor determined by RPLC in isocratic conditions (mobile phase: 65%MeOH/35% $AcONH_4$ buffer 25 mM); [c] structure in Fig. 1; [d] structure in Scheme 2; [e] Combretastatin A-4

General structure	cpd	X	R^1	R^2	MCF7 (IC_{50} nM)[a]	MDA-MB231 (IC_{50} nM)[a]	log k'[b]
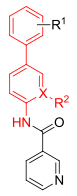	**29**	C	3',5'-diF	F	> 2500	> 2500	0.71±0.01
	30	N	3',5'-diF	-	> 2500	> 2500	0.67±0.01
	31	C	4'-F	$COOCH_3$	> 2500	> 2500	1.26±0.01
	32	C	4'-F	COOH	> 2500	> 2500	0.32±0.02
	33	C	4'-F	SO_2NH_2	>2500	> 2500	0.47±0.01
	34	C	4'-F	OCH_3	1200±400	> 2500	0.66±0.01
	35	C	4'-F	$NHCOCH_3$	> 2500	> 2500	0.32±0.02
	36	C	4'-F	CN	47±20	37±20	0.32±0.02
	37[b]	C	4'-F	CN	>2500	>2500	-

Table 3. Effects on antiproliferative activity (IC_{50}) of the replacements of *ortho*-nitro group in the biphenyl nicotinamide derivative **3**. [a] IC_{50} values (nM), coming from the mean of at least three independent experiments ± SEM, sampled in triplicate [b] Log of the capacity factor determined by RPLC in isocratic conditions (mobile phase: 65%MeOH/35% $AcONH_4$ buffer 25 mM); [c] 3,4,5-trimethoxybenzoyl analog (Scheme 1).

As shown by the IC_{50} values of the *ortho*-NO_2 derivatives in Table 2, the 3',5'-difluorinated biphenyl nicotinamide **3** displayed a noteworthy antiproliferative activity against MCF7 and MDA-MB231 cell lines (250 and 229 nM, respectively). Replacing the nicotinamide moiety with the positional isomer moieties, i.e. isonicotinamide (**22**) and picolinamide (**23**), resulted in a loss of activity. Interestingly, *N*-(4-ethoxy-2-nitrophenyl)nicotinamide (**4**), previously reported as apoptosis inducer in different cancer cell lines (e.g., human breast cancer T47D, ZR75-1 and colorectal DLD-1)[6] and re-synthesized in this study, proved to be almost equipotent with **3** in inhibiting proliferation in both human breast cancer cell lines MCF 7 and MDA-MB231.

A further investigation of the structure activity relationships was carried out by varying number and position of fluorine atoms (**24** and **25**) and replacing F with OCH_3 (**26** and **27**) on the distal phenyl ring. Within the limits of the chemical space examined, a net gain in the cell growth inhibition potency over compound **3** was observed with 4'-F (**24**) and 3'-OCH_3 (**27**) derivatives.

A different spatial geometry of the biphenyl moiety in **24** caused a drop of biological potency, as shown by the positional isomer **28** in which the distal 4'-F-phenyl is moved from *para* (in **24**) to *meta* position relative to NHCO.

The antiproliferative potency of the compounds in Table 2 appeared not dependent on the lipophilicity, as experimentally assessed by reversed phase HPLC (log *k*'). Indeed, the most active compounds **24** and **27** are almost isolipophilic (log *k*' ca. 0.8) with the less active compounds, whereas the most lipophilic derivative **22** (log *k*' 1.6) did not show any activity up to 2.5 μM concentration.

We attempted to replace in the hit compounds **3** and **24** the *ortho*-NO_2 substituent, which may result a toxicoforic group as demonstrated in several cases,[14],[15] with different substituents and bioisosters (Table 3). Most of these derivatives are not able to retain the activity expected for the OCH_3 congener **34**, and the CN congener **36** proved to be one of the most active compounds of the series, showing IC_{50} values comparable to those of **24** and

27. HPLC monitoring showed that the *ortho*-CN biphenyl nicotinamide derivative **36** is highly stable in PBS (100 mM, pH 7.4), remaining intact after 24 h incubation, and stable enough in 100% human serum (half-live *ca*. 12 h).

The activity drop of **37** with respect to **36** ultimately proved the superiority of the nicotinoyl over trimethoxybenzoyl moiety. Yet, for the series of compounds in Table 2, no correlation appeared to exist between the antiproliferative potency and lipophilicity.

A major outcome of this study was the evidence that the nitrile group can be a successful replacement of the nitro group, as demonstrated by the nanomolar antiproliferative potency of compound **36**. Actually, the number of nitrile-containing pharmaceuticals has recently increased[16] and the role in medicinal chemistry of this functional group has been deeply understood. The CN group should be biocompatible[17] and stable to metabolic transformation.[18] This short polarized triple bond,[19] smaller than a methyl group,[20] is able to penetrate narrow clefts, attaining polar interactions and HBs as acceptor [21] with amino acid side chains or water molecules.[19],[22] It is recognized that CN group/s may be introduced in bioactive molecules for improving ADME properties, but also for pharmacodynamic reasons (e.g., halogen bioisoster).[23]

To investigate the possible targets of the biphenyl nicotinamide derivatives, we started with examining the interference of compound **36** in the cell cycle progression of two human breast cancer cell lines, MCF-7 and MDA-MB-231, which differ for their proliferative potential. Cell cycle progression is perturbed by a variety of anticancer drugs, and investigating drug-dependent modifications can contribute to the phenotypic characterization of compounds under preclinical development.[24]

Cell-cycle changes induced by compound **36** on MCF7 and MDA-MB231 cells were investigated by the Operetta high-content imaging system, using a multiparametric approach to quantify DNA content (NuclearMask™ Blue Stain), DNA synthesis (EdU-positive cells), and mitotic cells (pHH3-positive cells). Nuclear DNA content evaluation is widely used for cell-cycle phase identification in flow cytometry as well as in high content imaging systems.[25],[26] MCF7 or MDA-MB231 cells growing in control (DMSO-treated) wells were stained with the nuclear dye after formaldehyde fixation and imaged using a 20x long working distance objective.

Harmony software was first used for image analysis (an example is shown for MCF7 cells in Figure 3A), and PhenoLOGIC algorithm was then applied to separate single cells from clumps. From the single cell results, a histogram of nuclear dye intensity sum was generated and the intensity corresponding to the center of the G1 peak determined. Based on this value, a histogram of normalized DNA (relative DNA content) was obtained from DMSO-treated wells on a per-plate basis and applied to all wells to identify sub-G1, G1, S, G2/M, and > G2/M cell populations (Figure 3B). DNA histograms for MCF7 cells treated with **36** or vinblastine at concentrations inducing similar growth inhibitory effects (80 and 5 nM, respectively) are shown in Figure 4 (inserts C and D). To provide a direct evaluation of cells in S-phase and to separate G2 from M populations, EdU incorporation and pHH3 expression were added to DNA content measurements, as shown in Figure 4E and 4F, respectively. In this way, the effect of **36** treatment on MCF7 cell cycle was investigated and compared to that of vinblastine, by identifying sub-G1, G1, S, G2, M, and > G2/M cell populations (Figure 3I and 3J).

Both **36** and vinblastine induced on MCF7 cells a dose-dependent accumulation of G2- and M-phase cell populations and a decrease of S-phase cells. However, unlike vinblastine, compound **36** induced also a G1 arrest at low doses (20-40 nM). Interestingly, both G1/G2 and M arrests were associated with cell number reduction (Figure 3 H) along with an increase of sub-G1 population, which appeared indicative of apoptosis. These results suggest that compound **36**, at low doses, behaves differently from vinblastine, its action likely depending upon activity on multiple pharmacological targets that seems engaged with increasing concentrations. The effects of **36** and vinblastine on MDA-MB231 cells were similar to those on MCF7 as far as cell cycle modifications are concerned, i.e. dose-dependent increase of G2 and M cells for both compounds, and additional G1 increase for **36** at low doses (data not shown). On a molar basis, however, vinblastine showed the same efficacy on the two cell lines, whereas **36** was almost twice more effective on MDA-MB231 cells. Overall, the divergent cell cycle status following low- and high-dose, along with the higher inhibitory potency of **36** on the p53-defective MDA-MB231 cells, supports a multiple target hypothesis for compound **36**, stimulating investigation on its mechanism of action.

On the basis of a structural analogy between compound **36** and the 6-chloro analog of **4**, a previously reported potent inhibitor of tubulin polymerization (IC_{50} 0.5 μM),[6] we considered of a certain interest to test a number of active biphenyl nicotinamides in a cell-free tubulin polymerization assay. The progression of tubulin polymerization was examined by monitoring the increase in fluorescence emission at 420 nm (excitation wavelength is 360 nm) for 1 h at 37 °C. Vinblastine and paclitaxel, two known microtubule-targeting agents acting as disassembly- and an assembly-promoter, respectively, were used as controls.[27] The effects on tubulin polymerization of three substances are shown in Figure 4 (i.e., **4** as reference inhibitor and its biphenyl analog **3**, as well as the potent antiproliferative compound **36**).

As expected, paclitaxel was a stabilizer of tubulin polymerization at 3 μM concentration, whereas vinblastine at the same concentration acted as an effective inhibitor of tubulin polymerization. The *ortho*-NO_2-phenyl nicotinamides **3** and **4** (Table 2) at 3 μM concentration displayed profiles similar to that of vinblastine, whereas the *ortho*-CN-phenyl nicotinamide **36**, a more potent antiproliferative agent (Table 3), did not show any appreciable effect on the progression of tubulin polymerization (profile similar to control). Concentration-dependent effects of **3** on tubulin polymerization, indicating the inhibitory potency at 0.03-3 μM concentrations, are shown in SI (Fig. S1).

Apparently, the inhibitory effect of the tested nicotinoyl anilides on tubulin polymerization *in vitro* do not relate with the antiproliferative activity.

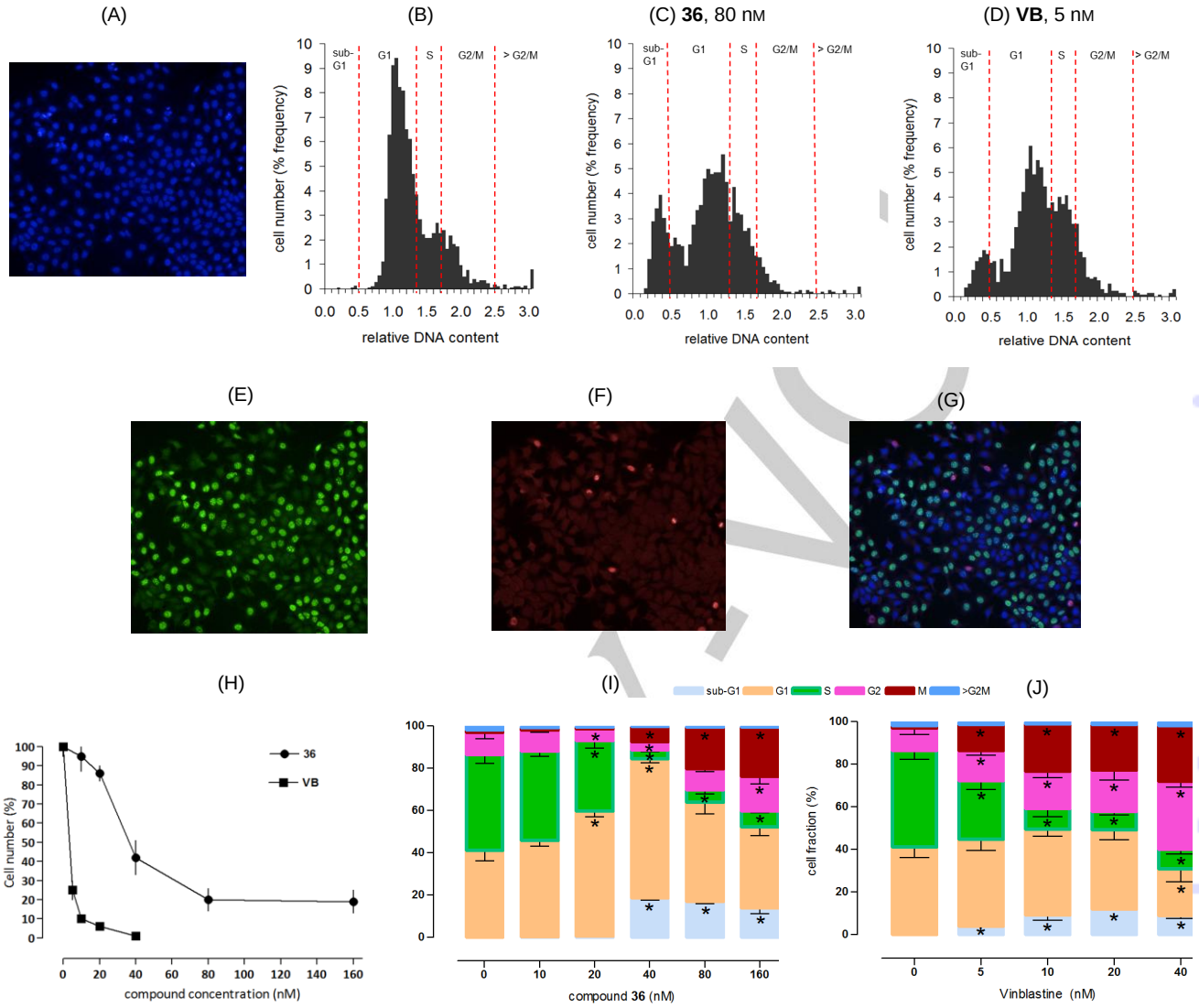

Figure 3. High-content cell cycle analysis. (A) Example image of vehicle-treated MCF7 cells with nuclei stained with NuclearMask™ Blue Stain. DNA content histograms of vehicle-treated MCF7 cells (B), and of cells treated with compound **36** (C) or vinblastine (VB) (D) at concentrations with similar cell number reduction effects. By using the PhenoLOGIC algorithm, cell populations were separated based on normalized DNA content: <0.5, subG1; 0.5-1.35, G1; 1.35-1.70, S; 1.70-2.5, G2/M; >2.5, >G2/M (red dotted lines). Representative images of vehicle-treated MCF7 cells stained with Alexa Fluor 488 (green, S-phase cells), and anti-pHH3 (red, M-phase cells) antibodies are shown in (E) and (F), respectively, while a merging image from (A), (E) and (F) is shown in (G). (I) and (J), vinblastine and **36** dose-response cell-cycle modifications determined using the multiparametric approach. (H) Effect of **36** or vinblastine treatment on cell number Values are the average of 5-8 technical replicates ± SD. * $P < 0.05$ *versus* vehicle-treated controls (Student's *t*-test, two-tailed distribution, two sample equal variance).

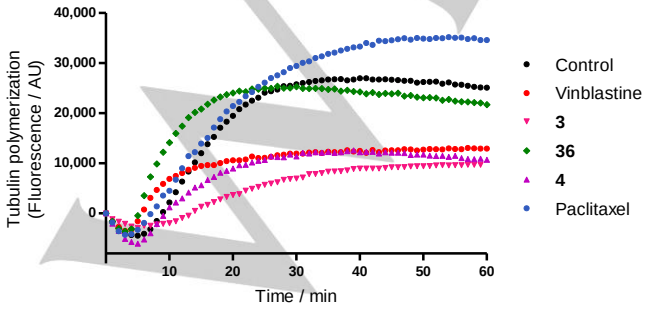

Figure 4. Effect of compounds **3**, **4** and **36** on tubulin polymerization (Cytoskeleton® kit).[28] Tubulin polymerization was monitored by the increase of fluorescence at 360 nm (excitation) and 420 nm (emission) for 1 h at 37 °C. All the compounds were tested at 3 µM concentration. Paclitaxel and vinblastine, at 3 µM concentration, were used as positive controls for tubulin polymerization inhibition and stabilization, respectively. Data points are means of triplicate experiments. The dose-response curve of compound **3** is reported as an example in support information (Figure 5.SI).

It is likely that the different behavior of the *N*-(2-nitrophenyl)nicotinamides **3** and **4** (inhibitors) with respect to the *N*-(2-cyanophenyl)nicotinamide derivative **36** (ineffective) may

be related to the molecular flatness, which in turn should depend upon the formation of intramolecular HB (IMHB) between the amide NH (HB donor) and the HB acceptor group in *ortho* position (NO_2 or CN).[28] In principle, IMHB formation should be more favored in the case of 2-NO_2 congeners (e.g., **3** and **4**), rather than in the case of 2-CN congeners (e.g., **36**). A broader and more in-depth SAR study can help in establishing whether and to what extent a more flat molecular geometry of the biphenyl nicotinamides, resulting from IMHB formation, can be causatively related to the inhibition of the tubulin polymerization.

Conclusion

A number of *N*-nicotinoyl biphenyl anilides were designed and synthesized, and two new potent *in vitro* antiproliferative agents (**24** and **27**) were identified. The need to replace in these compounds the potentially toxicoforic NO_2 group, while preserving their good antiproliferative activity, led to the synthesis of a second series of biphenyl nicotinamides. Among the investigated bioisosteric analogs, the nitrile-containing analog **36** proved to be almost equipotent with the corresponding nitro derivative **24**, showing nanomolar IC_{50} values against two breast tumor cell lines, MCF7 and MBA-MB231 (IC_{50} 47 and 37 nM, respectively). A cell-cycle progression analysis on MCF7 cells, accomplished through multiparametric automated microscopy, revealed a similar dose-dependent accumulation of G2- and M-phase cell populations and a decrease of S-phase for **36** and vinblastine, taken as reference drug. On the other hand, compound **36**, unlike vinblastine, induced also a G1 arrest at low doses (20-40 nM). Interestingly, G1/G2 and M arrests were associated with cell number reduction, along with an increase of sub-G1 population indicative of apoptosis. This finding suggests that **36**, at low concentrations, acts with a mechanism different from vinblastine. Moreover, compound **36** did not show inhibitory effects on tubulin polymerization. The possibility that the high antiproliferative activity of compound **36** is associated to a multi-target mechanism, which is appealing for a small molecule, deserves further pharmacological investigation.

Experimental Section

High analytical grade chemicals and solvents were purchased from commercial suppliers. When necessary, solvents were dried by standard techniques and distilled. After extraction from aqueous layers, the organic solvents were dried over anhydrous sodium sulfate. Thin layer chromatography (TLC) was performed on aluminum sheets pre-coated with silica gel 60 F254 (0.2 mm) (E. Merck). Chromatographic spots were visualized by UV light. Purification of crude compounds was carried out by flash column chromatography on silica gel 60 (Kieselgel 0.040−0.063 mm, E. Merck) or by preparative TLC on silica gel 60 F254 plates or crystallization. ^{1}H NMR spectra were recorded in DMSO-d_6 or $CDCl_3$ at 300 MHz on a Varian Mercury 300 instrument. Chemical shifts (δ scale) are reported in parts per million (ppm) relative to the central peak of the solvent. Coupling constant (J values) are given in hertz (Hz). Spin multiplicities are given as s (singlet), br s (broad singlet), d (doublet), t (triplet), dd (double doublet), dt (double triplet), or m (multiplet). LRMS (ESI) was performed with mass Q-TOF spectrometer (6530 mass Q-TOF Agilent, Palo Alto, CA). In all cases, spectroscopic data are in agreement with known compounds and assigned structures. Combustion analyses were performed by Eurovector Euro EA 3000 analyzer (Milan, Italy) and gave satisfactory results (C, H, N within 0.4% of calculated values).

Chromatographic settings. Purity determinations were carried out using a Zorbax 300SB-C18 4.6 x 250mm, with 5 µm size particles, built on a Waters double pump HPLC system in isocratic conditions. Injection volumes were 5 µL, flow rate was 1 mL/min, detection was performed with UV (λ=230 nm and 254 nm). Samples were prepared by dissolving 0.1 mg/mL of the solute in 10% (v/v) DMSO and 90% (v/v) methanol. Retention times (t_r) were measured at least from three separate injections, dead time (t_0) was the retention time of deuterated water. The mobile phase was filtered through a Nylon 66 membrane 0.45µm (Supelco, USA) before use.

General procedure for the Suzuki-Miyaura cross-coupling reaction:preparation of compounds **1A-12A** (Scheme 1).

A suspension of the chosen aniline (5.0 mmol), the appropriated boronic acid (7.5 mmol), and $Pd(PPh_3)_4$ (0.577 g, 0.50 mmol) in a aqueous solution 2M of K_2CO_3 (7.5 mL) and 1,4-dioxane (30 mL) was heated at 100 °C for 7 h under stirring. After cooling, the solvent was evaporated under vacuum to dryness and the obtained residue was treated with dichloromethane. The suspension was filtered on celite, or silica gel and the resulting residue was purified by chromatography.

3',5'-difluoro-3-nitro-[1,1'-biphenyl]-4-amine (**1A**):
Yield: 70%; ^{1}HNMR (300 MHz, DMSO-d_6) δ: 8.27 (d, J= 2.1 Hz, 1H), 7.82 (dd, J=2.2 Hz, J= 8.9 Hz, 1H), 7.61 (s br, 2H), 7.41 (d, J= 7.3 Hz, 2H), 7.16 (d, J=9.2 Hz, 1H), 7.09 (d, J=8.9 Hz, 1H); LRMS (ESI) *m/z* 249 [M-H]$^-$.

4'-fluoro-3-nitro-[1,1'-biphenyl]-4-amine (**2A**):
Yield: 65%; ^{1}H NMR (300 MHz, $CDCl_3$) δ: 8.32 (d, J= 2.2 Hz, 1H), 7.59 (dd, J=2.1 Hz, J= 8.6 Hz, 1H), 7.55 – 7.46 (m, 2H), 7.13 (t, J= 8.7 Hz, 2H) 6.89 (d, J= 8.7 Hz, 1H), 6.11 (s br, 2H); LRMS (ESI) *m/z* 231 [M-H]$^-$.

3'-fluoro-3-nitro-[1,1'-biphenyl]-4-amine (**3A**):
Yield: 70%; ^{1}H NMR (300 MHz, $CDCl_3$) δ: 8.37 (d, J= 2.2 Hz, 1H), 7.62 (dd, J= 2.2 Hz, J= 8.6 Hz, 1H), 7.44 – 7.30 (m, 3H), 7.03 (t, J= 8.9 Hz, 1H), 6.90 (d, J= 8.7 Hz, 1H), 6.15 (s br, 2H); LRMS (ESI) *m/z* 231 [M-H]$^-$.

4'-methoxy-3-nitro-[1,1'-biphenyl]-4-amine (**4A**):
Yield: 29%; ^{1}H NMR (300 MHz, $CDCl_3$) δ: 8.32 (d, J= 2.2 Hz, 1H), 7.60 (dd, J=2.2 Hz, J=8.6 Hz, 1H), 7.55 – 7.41 (m, 2H), 7.02 – 6.93 (m, 2H), 6.87 (d, J= 8.6 Hz, 1H), 6.07 (s br, 2H) 3.85 (s, 3H); LRMS (ESI) *m/z 243* [M-H]$^-$.

3'-methoxy-3-nitro-[1,1'-biphenyl]-4-amine (**5A**):
Yield: 60%; ^{1}H NMR (300 MHz, $CDCl_3$) δ: 8.38 (d, J= 2.2 Hz, 1H), 7.64 (dd, J= 2.2 Hz , J= 8.6 Hz, 1H), 7.37 (d, J= 7.9 Hz, 1H), 7.14 (d, J= 7.7 Hz, 1H), 7.09 – 7.06 (m, 1H), 6.89 (d, J= 8.6 Hz, 2H), 6.11 (s br, 2H), 3.87 (s, 3H); LRMS (ESI) *m/z* 243 [M-H]$^-$.

3,3',5'-trifluoro-[1,1'-biphenyl]-4-amine (**6A**):
Yield: 10%^{1}H NMR (300 MHz, $CDCl_3$) δ: 7.24 – 7.13 (m, 2H), 7.06 – 6.97 (m, 2H), 6.83 (dd, J= 8.3 Hz, J= 8.9 Hz, 1H), 6.76-6.67 (m, 1H), 3.86 (s br, 2H); LRMS (ESI) *m/z* 222 [M-H]$^-$.

5-(3,5-difluorophenyl)pyridin-2-amine (**7A**):
Yield: 70%; δ: ^{1}H NMR (300 MHz, $CDCl_3$) δ: 8.29 (d, J= 2.4 Hz, 1H), 7.62 (dd, J= 2.5 Hz, J= 8.5 Hz, 1H), 7.08 – 6.95 (m, 2H), 6.79-6.69 (m, 1H), 6.57 (d, J= 8.6 Hz, 1H), 4.58 (s br, 2H); LRMS (ESI) *m/z* 205 [M-H]$^-$.

Methyl 4-amino-4'-fluoro-[1,1'-biphenyl]-3-carboxylate (**8A**):
Yield: 17%; ^{1}H NMR (300 MHz, $CDCl_3$) δ: 8.06 (d, J= 2.3 Hz, 1H), 7.52-7.44 (m, 3H), 7.16 – 7.04 (m, 2H), 6.74 (d, J= 8.5 Hz, 1H), 5.78 (s br, 2H), 3.90 (s, 3H); LRMS (ESI) *m/z* 244 $[M-H]^-$.
4-amino-4'-fluoro-[1,1'-biphenyl]-3-sulfonamide (**9A**):
Yield: 35%; ^{1}H NMR (300 MHz, $CDCl_3$) δ: 7.97 (d, J= 2.2 Hz, 1H), 7.55 (dd, J= 2.2 Hz, J= 8.4 Hz, 1H), 7.51-7.44(m, 2H), 7.11 (t, J= 8.7 Hz, 2H), 6.88 (d, J= 8.4 Hz, 1H), 4.86 (s br, 4H). LRMS (ESI) *m/z* 265 $[M-H]^-$.
4'-fluoro-3-methoxy-[1,1'-biphenyl]-4-amine (**10A**):
Yield: 66%. ^{1}H NMR (300 MHz, $CDCl_3$) δ: 7.51 – 7.43 (m, 2H), 7.12–7.03 (m, 2H), 7.00–6.94 (m, 2H), 6.76 (d, J= 7.6 Hz, 1H), 3.92 (s, 3H), 3.86 (s br, 2H); LRMS (ESI) *m/z* 216 $[M-H]^-$.
4-amino-4'-fluoro-[1,1'-biphenyl]-3-carbonitrile (**11A**):
Yield: 79%; ^{1}H NMR (300 MHz, $CDCl_3$) δ: 7.59 – 7.48 (m, 2H), 7.47–7.38 (m, 2H), 7.16–7.05 (m, 2H), 6.81 (d, J= 8.5 Hz, 1H), 4.45 (s br, 2H); LRMS (ESI) *m/z* 211 $[M-H]^-$.
4'-fluoro-4-nitro-[1,1'-biphenyl]-3-amine (**12A**):
Yield: 28%; ^{1}H NMR (300 MHz, $CDCl_3$) δ: 8.18 (d, J= 8.9 Hz, 1H), 7.60 – 7.52 (m, 2H), 7.15 (t, J= 8.7, 2H), 6.93 (d, J=1.8 Hz, 1H), 6.89 (dd, J= 1.9 Hz, J= 8.9 Hz, 1H), 6.15 (s br, 2H). LRMS (ESI) *m/z* 231 $[M-H]^-$.
Synthesis of *N*-(4'-fluoro-4-nitro-[1,1'-biphenyl]-3-yl)acetamide (**13 A**):
0.86 mmol (0,200 g) of 12A were dissolved in 4 ml of dry THF and 1.73 mmol (0.123 ml) of acetyl chloride were added. The mixture was stirred for 72 h and then poured in a NH_4Cl saturated aqueous solution. The obtained precipitate was filtered and dried under vacuum.
Yield: 66%; ^{1}H NMR (300 MHz, $CDCl_3$) δ: 10.49 (s br, 1H), 9.04 (d, J= 2.0 Hz, 1H), 8.29 (d, J= 8.8 Hz, 1H), 7.68 – 7.60 (m, 2H), 7.35 (dd, J= 2.0 Hz, J= 8.8 Hz, 1H), 7.17 (t, J=8.7, 2H), 2.32 (s, 3H); LRMS (ESI) *m/z* 273 $[M-H]^-$.
Synthesis of *N*-(4-amino-4'-fluoro-[1,1'-biphenyl]-3-yl)acetamide (**14A**):
0.36 mmol (0.100g) of 13 A were dissolve in 5 ml of MeOH and 1,8 mmol (0.406g) of $SnCl_2$ were added and the mixture was stirred for 24h. The mixture was evaporated and purified by chromatography (CH_2Cl_2 as eluent) obtaining the desired product.
Yield: 87%; ^{1}H NMR (300 MHz, DMSO-d_6) δ: 9.46 (s br, 1H), 7.60–7.46 (m, 2H), 7.33–7.16 (m, 4H), 7.09 (s, 1H), 6.92 (s br, 2H), 2.06 (s, 3H); LRMS (ESI) *m/z* 245 $[M+H]^+$.
Synthesis of compounds **3, 22-31, 33-37**.
The intermediate anilines **1A-12A** and **14A** (1 mmol) were dissolved in dry dioxane (0.1 M) and then nicotinoyl chloride hydrochloride (3 mmol), DMAP (1 mmol) and TEA (6 mmol) were added. The mixture was refluxed for 18 hours. After cooling the obtained precipitate was removed by filtration. The filtrate was evaporated and the residue was purified by crystallization or silica column chromatography.
To synthesize compound **23** the commercially available isonicotinoyl chloride was used for the reaction with compound 1A in the same conditions.
For compound **22** and **37** the starting aryloyl acid (1.5 mmol) was suspended under argon in thionyl chloride (2.0 mL) and heated under reflux for 2h. The unreacted excess of thionyl chloride was removed under nitrogen flow to afford the corresponding aryloyl chloride. The solid obtained was used without further purification for the reaction with the aniline **1A** and **11A**, respectively, in the condition described above.
N-(3',5'-difluoro-3-nitro-[1,1'-biphenyl]-4-yl)nicotinamide (**3**):
Yellow solid (yield: 16%.); Mp:188-190 °C; ^{1}H NMR (300 MHz, DMSO-d_6) δ: 11.00 (s br, 1H), 9.12 (d, J= 1.7 Hz, 1H), 8.85 – 8.75 (m, 1H), 8.35 (d, J= 2.0 Hz, 1H), 8.33 – 8.26 (m, 1H), 8.15 (dd, J= 2.0 Hz, J= 8.6 Hz, 1H), 7.82 (d, J= 8.5 Hz, 1H), 7.65-7.56 (m, 3H), 7.35-7.26 (m,1H); LRMS (ESI) *m/z* 354 $[M-H]^-$.
N-(3',5'-difluoro-3-nitro-[1,1'-biphenyl]-4-yl)picolinamide (**22**):
Yellow solid (yield: 27%); Mp>250 °C; ^{1}H NMR (300 MHz, DMSO-d_6) δ: 12.27 (s br, 1H), 8.82 - 8.74 (m, 2H), 8.53 (d, J= 2.1 Hz, 1H), 8.27 – 8.19 (m, 2H), 8.16-8.07 (m, 1H), 7.79 – 7.69 (m, 1H), 7.66-7.56 (m, 2H), 7.35-7.25 (m, 1H); LRMS (ESI) *m/z* 354 $[M-H]^-$.
N-(3',5'-difluoro-3-nitro-[1,1'-biphenyl]-4-yl)isonicotinamide. (**23**):
Yellow solid (yield: 17%); Mp:233-235 °C; ^{1}H NMR (300 MHz, $CDCl_3$) δ: 11.48 (s br, 1H), 9.11 (d, J= 8.9 Hz, 1H), 8.93 – 8.86 (m, 2H), 8.50 (d, J= 2.2 Hz, 1H), 7.94 (dd, J= 2.2 Hz, J= 8.9 Hz, 1H), 7.88 – 7.80 (m, 2H), 7.19 – 7.09 (m, 2H), 6.88 (t, J= 8.7 Hz, 1H); LRMS (ESI) m/z 354 $[M-H]^-$.
N-(4'-fluoro-3-nitro-[1,1'-biphenyl]-4-yl)nicotinamide (**24**):
Yellow solid (yield: 50%); Mp:177-178 °C; ^{1}H NMR (300 MHz, $CDCl_3$) δ: 11.39 (s br, 1H), 9.28 (d, J= 2.3 Hz, 1H), 9.05 (d, J= 8.8 Hz, 1H), 8.86 (dd J= 1.6 Hz, J= 4.8 Hz, 1H), 8.48 (d, J= 2.2 Hz, 1H), 8.35 – 8.25 (m, 1H), 7.93 (dd, J= 2.2 Hz, J= 8.8 Hz, 1H), 7.60 (dd, J= 5.2 Hz , J=8.8 Hz, 2H), 7.51 (dd, J= 4.8 Hz, J= 8.0 Hz, 1H), 7.19 (t, J= 8.6 Hz, 2H); LRMS (ESI) *m/z* 336 $[M-H]^-$.
N-(3'-fluoro-3-nitro-[1,1'-biphenyl]-4-yl)nicotinamide. (**25**):
Yellow solid (yield: 58%); Mp:185-186 °C; ^{1}H NMR (300 MHz, DMSO-d_6) δ: 10.98 (s br, 1H), 9.12 (d, J= 1.6 Hz, 1H), 8.81 (dd, J =1.6 Hz, J= 4.8 Hz, 1H), 8.33- 8.25 (m, 2H), 8.12 (dd, J=2.2 Hz, J=8.5 Hz, 1H), 7.81 (d, J= 8.5 Hz, 1H), 7.71 – 7.50 (m, 4H), 7.32 – 7.20 (m, 1H); LRMS (ESI) *m/z 336* $[M-H]^-$.
N-(4'-methoxy-3-nitro-[1,1'-biphenyl]-4-yl)nicotinamide (**26**):
Yellow solid (yield: 42%) ; Mp:182-183 °C; ^{1}H NMR (300 MHz, $CDCl_3$) δ: 11.37 (s br, 1H), 9.27 (d, J= 1.8 Hz, 1H), 9.01 (d, J= 8.8 Hz, 1H), 8.85 (dd J= 1.6 Hz, J= 4.8 Hz, 1H), 8.47 (d, J= 2.2 Hz, 1H), 8.29 (ddd J=1.7 Hz, J=2.3 Hz, J=8.0 Hz, 1H), 7.93 (dd, J= 2.2 Hz, J=8.8 Hz,1H), 7.57 (d, J= 8.9 Hz, 2H), 7.51 (dd, J= 4.8 Hz, J= 8.0 Hz, 1H), 7.02 (d, J= 8.8 Hz, 2H), 3.88 (s, 3H); LRMS (ESI) *m/z* 348 $[M-H]^-$.
N-(3'-methoxy-3-nitro-[1,1'-biphenyl]-4-yl)nicotinamide (**27**):
Yellow solid (yield: 73%); Mp:154-155 °C; ^{1}HNMR (300 MHz, $CDCl_3$) δ: 11.40 (s br, 1H), 9.28 (d, J= 2.2 Hz, 1H), 9.04 (d, J= 8.8 Hz, 1H), 8.85 (d, J= 3.3 Hz, 1H), 8.52 (d, J= 2.2 Hz, 1H), 8.30 (d, J= 7.7 Hz, 1H), 7.97 (dd, J= 1.9 Hz, J= 8.8 Hz, 1H), 7.51 (dd, J=4.9 Hz, J= 7.9 Hz, 1H), 7.42 (t, J= 7.9 Hz, 1H), 7.23-7.19 (m, 1H), 7.14 (s, 1H), 6.97 (d, J= 8.5 Hz, 1H), 3.90 (s, 3H); LRMS (ESI) *m/z* 348 $[M-H]^-$.
N-(4'-fluoro-4-nitro-[1,1'-biphenyl]-3-yl)nicotinamide (**28**):
Yellow solid (yield: 10%); Mp:190-191 °C; ^{1}H NMR (300 MHz, DMSO-d_6) δ: 10.98 (s br, 1H), 9.12 (d, J= 1.8 Hz, 1H), 8.79 (dd, J=1.8 Hz, J= 4.7 Hz 1H), 8.30 (dt, J= 1.8 Hz, J= 8.2 Hz, 1H), 8.09-8.04 (m, 2H), 7.82-7.78 (m, 2H), 7.71 (dd, J=1.8 Hz, J= 8.8 Hz, 1H), 7.60 (dd, J=5.2 Hz, J= 8.2 Hz, 1H) 7.39-7.33 (m, 2H). LRMS (ESI) *m/z* 336 $[M-H]^-$ . .
N-(3,3',5'-trifluoro-[1,1'-biphenyl]-4-yl)nicotinamide (**29**):
White solid (yield: 30%); Mp:239-240 °C; ^{1}H NMR (300 MHz, $CDCl_3$) δ: 9.15 (s, 1H), 8.83 (d, J= 4.8 Hz, 1H), 8.56 (t, J= 8.3 Hz, 1H), 8.24 (d, J= 8.2 Hz, 1H), 8.08 (s, 1H), 7.54 – 7.46 (m, 1H), 7.45 – 7.34 (m, 2H), 7.12-7.05 (m, 2H), 6.86-6.76 (m, 1H); LRMS (ESI) *m/z* 327 $[M-H]^-$.
N-(5-(3,5-difluorophenyl)pyridin-2-yl)nicotinamide (**30**):
White solid (yield: 12%); Mp:181-182 °C; ^{1}H NMR (300 MHz, DMSO-d_6) δ: 11.26 (s br, 1H), 9.14 (s, 1H), 8.82 (s, 1H), 8.75 (d, J= 3.3 Hz, 1H), 8.35 (d, J=8.0 Hz, 1 H), 8.27 (s, 2H), 7.61-7.50 (m, 3H), 7.31-7.18 (m, 1H); LRMS (ESI) *m/z* 310 $[M-H]^-$.
Methyl 4'-fluoro-4-(nicotinamido)-[1,1'-biphenyl]-3-carboxylate(**31**):
White solid (yield: 6%); Mp:189-190 °C; ^{1}H NMR (300 MHz, $CDCl_3$) δ: 12.19 (s br, 1H), 9.32 (d, J=2.0 Hz, 1H), 8.98 (d, J= 8.8 Hz, 1H), 8.81 (d, J= 4.8 Hz, 1H), 8.38 – 8.31 (m, 1H), 8.29 (d, J= 2.3 Hz, 1H), 7.82 (dd, J=2.3 Hz, J= 8.8 Hz, 1H), 7.62 – 7.54 (m, 2H), 7.48 (dd, J=4.8 Hz, J= 8.0 Hz, 1H), 7.16 (t, J= 8.7 Hz, 2H), 4.01 (s,3H); LRMS (ESI) m/z 349 $[M-H]^-$.
N-(4'-fluoro-3-sulfamoyl-[1,1'-biphenyl]-4-yl)nicotinamide (**33**):

White solid (yield: 15%); Mp>250 °C; ^{1}H NMR (300 MHz, DMSO-d_6) δ: 12.48 (s br, 1H), 9.21 (s, 1H), 8.82 (s, 1H), 8.45 – 8.37 (m, 1H), 8.03 (s, 2H), 7.85 – 7.75 (m, 3H), 7.65 (s, 2H), 7.39 – 7.22 (m, 3H); LRMS (ESI) m/z 370 [M-H]$^-$

N-(4'-fluoro-3-methoxy-[1,1'-biphenyl]-4-yl)nicotinamide (**34**):

White solid (yield: 33%); Mp:139-140 °C; ^{1}H NMR (300 MHz, DMSO-d_6) δ: 9.14 (d, J= 1.7 Hz, 1H), 8.80 (dd, J=1.7 Hz, J=4.8 Hz, 1H), 8.58 (s , 1H), 8.55 (s, 1H), 8.29 – 8.21 (m, 1H), 7.58 – 7.52 (m, 2H), 7.47 (dd, J= 4.9 Hz, J= 7.9 Hz, 1H), 7.24 – 7.19 (m, 1H), 7.17 – 7.08 (m, 3H), 4.01 (s,3H); LRMS (ESI) *m/z* 321 [M-H]$^-$.

N-(3-acetamido-4'-fluoro-[1,1'-biphenyl]-4-yl)nicotinamide (**35**):

White solid (yield: 25%); Mp:204-205 °C; ^{1}HNMR (300 MHz, $CDCl_3$) δ: 9.74 (s br, 1H), 9.20 (s, 1H), 8.74 (s br, 1H), 8.46 (s, 1H), 8.18-8.14 (m, 1H), 7.70 (d, J= 8.2 Hz, 1H), 7.35-7.27 (m, 2H), 7.24-7.22 (m, 2H), 7.01 (t, J= 8.75 Hz, 2H), 2.13 (s, 3H); LRMS (ESI) *m/z* 348 [M-H]$^-$.

N-(3-cyano-4'-fluoro-[1,1'-biphenyl]-4-yl)nicotinamide (**36**):

White solid (yield: 47%); Mp:223-224 °C; ^{1}H NMR (300 MHz, DMSO-d_6) δ: 9.22 (d, J= 2.3 Hz, 1H), 8.86 (dd, J= 1.6 Hz, J= 4.8 Hz, 1H), 8.64 (d, J= 8.7 Hz, 1H), 8.35 (s, 1H), 8.28 – 8.21 (m, 1H), 7.88 – 7.79 (m, 2H), 7.57-7.47 (m, 3H), 7.22-7.14 (m, 1H); LRMS (ESI) *m/z* 316 [M-H]$^-$.

N-(3-cyano-4'-fluoro-[1,1'-biphenyl]-4-yl)-3,4,5-trimethoxybenzamide (**37**):

White solid (yield: 20%); Mp:220-221 °C; ^{1}H NMR (500 MHz, DMSO-d_6) δ: 10.55 (s br, 1H), 8.19 (d, J= 2.2 Hz, 1H), 8.04 (dd, J= 2.3 Hz, J= 8.5 Hz, 1H), 7.86 – 7.80 (m, 2H), 7.63 (d, J= 8.5 Hz, 1H), 7.34 (s, 3H), 7.33 – 7.30 (m, 1H), 3.86 (s, 6H), 3.74 (s, 3H); LRMS m/z 405 [M-H]$^-$.

Synthesis of 4'-fluoro-4-(nicotinamido)-[1,1'-biphenyl]-3-carboxylic acid (**32**) 0.1 mmol (0.035 g) of compound 11 were dissolved in 4 mL of a mixture THF/water 3:1 and 0.1 mmol (0.003g) of LiOH were added. After 3 h the mixture was evaporated and the residue was treated with HCl 1N (5 mL) . The obtained precipitate was filtered and washed with water. White solid (yield: 55%); Mp>250 °C; ^{1}H NMR (300 MHz, DMSO-d_6) δ: 13.91 (s br, 1H), 12.29 (s br, 1H), 9.14 (s, 1H), 8.81 (s, 1H), 8.70 (d, J= 8.7 Hz, 1H), 8.36 – 8.23 (m, 2H), 7.97 (d, J= 8.0 Hz, 1H), 7.79 – 7.68 (m, 2H), 7.68 – 7.56 (m, 1H), 7.30 (t, J= 8.7 Hz, 2H); LRMS (ESI) m/z 335.0 [M-H]$^-$

Pharmacological assays

Tumor Cell Lines and *In Vitro* Growth Inhibition Assay:

Two human tumor cell lines of breast MCF7 and MDA-MB 231 were obtained from the National Cancer Institute, Biological Testing Branch (Frederick, MD, USA). The cell lines MCF7 and MDA-MB231 were maintained in the logarithmic phase at 37 °C in a 5% CO_2 humidified air in RPMI 1640 medium supplemented with 10% fetal calf serum and respectively with, 1% glutamine (200 mM), 1% penicillin and streptomycin (100 U/mL and 0.1 mg/mL) for MCF7 and 1,5% glutamine (200 mM), 2% penicillin and streptomycin (100 U/mL and 0.1 mg/mL) and 1% Na Pyruvate (100 mM) for MDA-MB231. The growth-inhibitory effect of the compounds under investigation was evaluated by using the Sulforhodamine-B (SRB) assay.[29]

Briefly, cells were seeded into 96-well microtiter plates in culture medium (100 µL) at a plating density of 5000 and 10000 cells/well to MCF-7 and MDA-MB-231 respectively. After seeding, microtiter plates were incubated at 37 °C for 24 h prior to addition of the compounds. After 24 h, samples of each cell line were fixed in situ with cold trichloroacetic acid (TCA), to represent a measurement of the cell population at the time of compound addition. The compounds to be tested (the stock solution was prepared at a concentration of 1 mM in DMSO) were diluted freshly in culture medium to the desired final concentrations (2.5–0.002 µM). After the addition of different compound concentrations to triplicate wells, the plates were further incubated at 37 °C for 72 h. Cells were fixed in situ by the slow addition of cold TCA (50 µL, 50% w/v, final concentration 10%) and incubated for 1 h at 4 °C. The supernatant was discarded, and the plates were washed four times with tap water and air-dried. Sulforhodamine- B solution (100 µL, 0.4% w/v, in 1% acetic acid) was added to each well, and plates were incubated for 30 min at room temperature. After staining, unbound dye was removed by washing five times with acetic acid (1 %), and the plates were air-dried. Bound stain was then solubilized in 10 mM 2-amino-2-(hydroxymethyl)-1,3-propanediol (Trizma base), and the absorbance was read on an automatic plate reader at 570 nm. The compound concentration able to inhibit cell growth by 50% (IC_{50} ± SD) was then calculated from semilogarithmic dose–response plots.

High-content cell cycle analysis

Treatment-induced modifications of cell cycle phases were investigated using the high-content imaging system Operetta (Perkin Elmer Life Sciences, Boston, MA), along with Harmony software and PhenoLOGIC machine learning, according to a method recently described by Massey AJ.[26] Briefly, MCF7 or MDA-MB231 cells in complete culture medium were seeded (4500 and 3000 cells/well, respectively) in a 96-well collagen-coated plate (Perkin Elmer), allowed to attach for 24 h in normal humified atmosphere supplemented with 5% CO_2, and then treated in the same conditions for further 24 h with different concentrations of freshly dissolved compounds. Cells were labelled with 10 µM (final concentration/well) 5-ethynyl-2'-deoxyuridine (EdU) for 30 min. After EdU incubation, media was removed immediately prior to fixation of adherent cells with formaldehyde 3.7% (v/v) in PBS at room temperature for 15 min. Cells were washed twice with PBS and permeabilized with Triton X-100 (Promega) for 15 min at room temperature. After two washes with PBS, incorporated EdU was detected with Alexa Fluor 488 by a Click-iT® EdU HCS Assay (C10350, Life Technologies) according to the manufacturer's recommended procedure. For phospho-histone H3 Ser28 detection, cells were incubated with 3% (w/v) bovine serum albumin (BSA) overnight at 4 °C, and then incubated for 1 h at room temperature in the dark with the anti-Phospho-Histone H3 primary antibody (Anti-Phospho-Histone H3 pSer28, clone HTA28, SIGMA), 2 µg/ml final concentration in BSA 3%. After three washes with 0.05% Tween® 20, cells were incubated with the secondary antibody (Alexa Fluor® 647 Goat anti-Rat IgG, ThermoFisher Scientific), 10 µg/ml final concentration in BSA 3%, for 1 h at room temperature in the dark. Following additional three washes with 0.05% Tween® 20, nuclear staining was performed for 15 min at room temperature in the dark by NuclearMask™ Blue Stain (Life Technologies), 100 µL/well. Finally, following two PBS washes, cells were imaged with an Operetta high-content imaging system (Perkin-Elmer) using a 20x long working distance objective. Typically, 10 fields per well were imaged which equated to approximately 3000 cells/well.

Analysis sequence. Image acquisition and data analysis were performed by using the Harmony ® Image Analysis Software with PhenoLOGIC (Perkin-Elmer, Inc. MA, USA). Automated analysis was performed to obtain as readout the total number of cells (for information and quality control) and DNA content on a single-cell basis (nuclear mask intensity sum). From the single cell results a histogram of nuclear mask sum was generated (Excel software) and the intensity corresponding to the center of the G1 peak determined. Based upon this value, a histogram of normalized DNA (relative DNA content) was obtained from vehicle-treated wells on a per-plate basis and applied to all wells to identify sub-G1, G1, S, G2/M, and > G2/M cell populations. Multiparametric analysis of cell-cycle was then performed by using relative DNA content values along with mean marker intensity values of EdU-positive and PHH3-

positive cells to specifically identify sub-G1, G1, S, G2, M, and > G2/M cells.

Statistical analysis

To determine concentration-dependent cell-cycle modifications, comparisons were made between each dose and the respective vehicle-only control. The cell fraction was calculated for each sample and paired two-tailed Student's *t*-test (two sample equal variance, $P < 0.05$) was used to determine the significance of the response. Values represent the means ± SD of 5-8 replicates.

***In vitro* tubulin polymerization assay**

A number of selected compounds were tested at 3 μM concentration in a tubulin polymerization assay kit (Cytoskeleton Inc., Denver, CO, USA). Lyophilized tubulin (Cytoskeleton #T240) was used to evaluate the tubulin polymerization inhibiting activity. Vinblastine and paclitaxel at 3.0 μM were used as positive controls for tubulin polymerization inhibition and stabilization, respectively. All compounds were dissolved in DMSO and further diluted with sterile water to obtain a maximum DMSO concentration of 0.1%, which was used as solvent control. Polymerization was monitored by fluorescence enhancement due to the incorporation of a fluorescent reporter into microtubules as polymerization occurs. In a 96 well plate, to a 0.5 μL of a 100x stock solution of each compound, 49.5 μL of supplemented tubulin supernatant were added. Incubation was done in a temperature-controlled Multi-label Microplate Fluorimeter, equipped with filters for excitation at 340-360 nm and emission at 420-460 nm (Victor 3 Model 1420-01296, Perkin-Elmer, Inc. MA, USA) at 37 °C, and fluorescence was measured at 460 nm every minute for 60 min according the recommended procedures.[30]

Acknowledgements

The authors would like to thank Giovanni Dipinto (Department of Pharmacy-Drug Sciences, University of Bari) for the assistance in Q-TOF Mass Spectrometry. The financial support by the University of Bari Aldo Moro is gratefully acknowledged.

Keywords: Nicotinoyl anilides, Antiproliferative assay, High-content cell cycle analysis, MCF-7 and MDA-MB231 tumor cell lines.

References:

[1] D. W. Lee, Y-S. Choi, S. Y. Jee, M-Y. Lee, S. Y. Jeon, B. Ku, S. Kim, S. H. Yi, D-H. Nam, *Anal. Chem*. **2014,** *86*, 535-542.

[2] R. Zang, D. Li, I-C. Tang, J. Wang, S-T. Yang, *Int. J. Biotech. Well. Indus.* **2012**, *1*, 31-51.

[3] R. Z. Pellicani, A. Stefanachi, M. Niso, A. Carotti, F. Leonetti, O. Nicolotti, R. Perrone, F. Berardi, S. Cellamare, N. A. Colabufo, *J. Med. Chem.* **2012**, *55*, 424-436.

[4] P. Tardia, A. Stefanachi, M. Niso, D.A. Stolfa,; G. F. Mangiatordi, D. Alberga, O. Nicolotti, G. Lattanzi, A. Carotti, F. Leonetti, R. Perrone, F. Berardi, A. Azzariti, N. A. Colabufo, S. Cellamare. *J Med Chem.* **2014**, *57*, 6403–6418.

[5] a) P. D. W. Eckford; F. J. Sharom, *Chem. Rev*. **2009**,*109*, 2989–3011; b) B. C. Baguley, *Methods Mol. Biol.* **2010**, *596*, 1–14

[6] S. X. Cai, B. Nguyen, S. Jia, J.Herich, J. Guastella, S. Reddy, B. Tseng, J. Drewe, S. Kasibhatla, *J. Med. Chem.* **2003**, *46*, 2474–2481.

[7] T. Suzuki, M. N. Ahmed Khan, H. Sawada, E. Imai, Y .Itoh, K. Yamatsuta, N. Tokuda, J. Takeuchi, T. Seko, H. Nakagawa, N. Miyata, *J. Med. Chem*. **2012**, *55*, 5760–5773.

[8] M. E. Kort, R. N. Atkinson, J. B. Thomas, I. Drizin, M. S. Johnson, M. A. Secrest, R. J. Gregg, M. J. C. Scanio, L. Shi, A. H. Hakeem, M. A. Matulenko, M. L. Chapman, M. J. Krambis, D. Liu, C.-C. Shieh, X. Zhang, G. Simler, J. P. Mikusa, C. Zhong, S. Joshi, P. Honore,; R. Roeloffs, S. Werness, B. Antonio, K. C. Marsh, C.R. Faltynek, D. S. Krafte, M.F. Jarvis, B. E. Marron, *Bioorg. Med. Chem. Lett.* **2010**, *20*, 6812–6815.

[9] A. B. Eldrup, F. Soleymanzadeh,; S. J. Taylor, I. Muegge, N. A. Farrow, D. Joseph, K. McKellop, C. C. Man, A. Kukulka, S. De Lombaert, *J. Med. Chem.* **2009**, *52*, 5880–5895.

[10] J. L. Methot,; P. K. Chakravarty, M. Chenard, J. Close, J. C. Cruz, W. K. Dahlberg, J. Fleming, C. L. Hamblett, J. E. Hamill, P. Harrington, A. Harsch,; R. Heidebrecht, B. Hughes, J. Jung, C.M. Kenific, A. M. Kral, P.T. Meinke, R. E. Middleton, N. Ozerova, D.L. Sloman, M. G. Stanton, A. A. Szewczak, S. Tyagarajan, D. J. Witter, J. P. Secrist,; T. A. Miller, *Bioorg. Med. Chem. Lett.* **2008**, *18*, 973–978.

[11] C. Reichwalda, O. Shimonyb, N. Sacerdoti-Sierrab, C. L. Jaffeb, C. Kunicka, *Bioorg. Med. Chem. Lett.* **2008**, *18*, 1985–1989.

[12] V. J. Huber, M. Tsujita, T. Nakada, *Bioorg. Med. Chem*. **2009,** *17*, 411–417.

[13] National Center for Biotechnology Information. PubChem Compound Database; CID=279877, https://pubchem.ncbi.nlm.nih.gov/compound/279877 (accessed Dec 30, 2015).

[14] G. F.Smith,. *Prog Med Chem*, **2011**, *50*,1–47.

[15] V. Purohit, A. K. Basu, *Chem Res Toxicol*, **2000**, *13*, 673-92.

[16] F. F. Fleming, L. Yao, P. C. Ravikumar, L. Funk, B. Shook, *J. Med. Chem.* **2010**, *53*, 7902–7917

[17] a) S. T. Murphy, H. L. Case, E. Ellsworth, S. Hagen, M. Huband, T. Joannides, C. Limberakis, K. R. Marotti, A. M. Ottolini, M. Rauckhorst, J. Starr, M. Stier, C. Taylor, T. Zhu, A. Blaser, W. A. Denny, G. L. Lu, J. B. Smaill, F. Rivault, *Bioorg. Med. Chem.Lett.* **2007**, *17*, 2150–2155. b) B. Markus, C.-H. Kwon, *J. Pharm. Sci.* **1994**, *83*, 1729–1734.

[18] a) M. J. Boyd, S. N. Crane, J. Robichaud, J. Scheigetz, W. C. Black,; N. Chauret, Q. Wang, F. Masse, R. M. Oballa, *Bioorg. Med. Chem. Lett.* **2009**, *19*, 675–679. (b) A. W. Patterson, W. J. L. Wood, M. Hornsby, S. Lesley, G. Spraggon, J. A.Ellman, *J. Med. Chem*. **2006**, *49*, 6298–6307.

[19] J.-Y. Le Questel, M. Berthelot, C. Laurence, *J. Phys. Org. Chem*. **2000**, *13*, 347–358.

[20] E. L. Eliel, S. H. Wilen, L. N. Mander, *Stereochemistry of Organic Compounds*, Wiley, **1994**, p. 696–697.

[21] N. Teno, T. Miyake, T. Ehara, O. Irie, J. Sakaki, O. Ohmori, H. Gunji, N. Matsuura, K. Masuya, Y. Hitomi, K. Nonomuraa, M. Horiuchia, K. Gohdaa, A. Iwasakia, I. Umemuraa, S. Tadaa, M. Kometania, G. Iwasakia,; S. W. Cowan-Jacobb, M. Missbachb, R. Lattmannb, C. Betscharta, *Bioorg. Med. Chem. Lett*. **2007**, *17*, 6096–6100.

[22] a) C. Laurence, K. A Brameld,. J. Graton, J.-Y. Le Questel, E. Renault, *J. Med. Chem.* **2009**, *52*, 4073–4086. (b) A. Allerhand, P.Schleyer, von Rague, *J. Am. Chem. Soc*. **1963**, *85*, 866–870.

[23] T. Nogrady, D. F. Weaver, *Medicinal Chemistry: A Molecular and Biochemical Approach*, Oxford University Press, **2005**, p. 22.

[24] F. Gasparri, A. Ciavolella, A. Galvani. *Adv Exp Med Biol* **2007**, *604*, 137-148.

[25] G. K. Chan, T. L. Kleinheinz, D. Peterson, J. G. Moffat. *PLoS One* **2013**, *8(5)*, e63583.

[26] A. J. Massey. *PLoS One* **2015**, *10*, e0134306.

[27] B. T. Castle, S. McCubbin, L. S. Prahl, J. N. Bernens, D. Sept, D. J. Odde. *Mol Biol Cell* **2017**, doi: 10.1091/mbc.

[28] A. Stefanachi, G.F. Mangiatordi, P. Tardia, D. Alberga, F. Leonetti, M. Niso, N.A. Colabufo, C. Adamo, O. Nicolotti, S. Cellamare. *Chem. Biol. Drug Des.* **2016**, *88*, 820-831.
[29] http://www.cytoskeleton.com/bk011p
[30] V. Vichai, K. Kirtikara. *Nature Protocols* **2006**, *1*, 1112-1116.

Entry for the Table of Contents

Insert graphic for Table of Contents here.

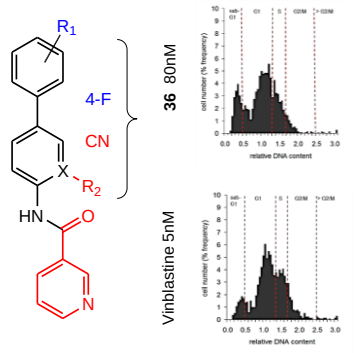

Insert text for Table of Contents here.

A screening of a small library of trimethoxybenzoic and nicotinic acid anilides, previously studied as P-gp modulators, allowed us to identify some *N*-biphenyl nicotinoyl anilides showing very interesting antiproliferative activities. The next hit refinement by a biosisosteric approach, led us to observe potent antiproliferative activity of the cyano derivative **36** against MCF7 and MDA-MB231 cells lines.